



OPEN

Study on the growth process and water consumption characteristics of forage oats based on aquacrop model

Yuchao Chen^{1,2,3}, Bing Xu^{1,2}✉, Guoshuai Wang^{1,2}✉, Delong Tian^{1,2}, Lingyun Xu^{1,2,3}, Jie Zhou^{1,2,3}, Xiangyang Miao^{1,2} & Xianyue Li³

The water resources in the Yellow River irrigation area of Inner Mongolia are tight, and the utilization efficiency of farmland irrigation water is low. The shallow buried drip irrigation mode is adopted in the local oat double-cropping planting, but its growth and development and water consumption process are not clear. In-depth study of the growth and water consumption of forage oats in the whole growth period under this model is very important for optimizing irrigation system, improving water use efficiency and increasing crop yield. A field experiment was conducted in Tumotezuoqi, Inner Mongolia. The database was established according to the meteorological-soil-crop-irrigation factors in 2022 and 2023, and the AquaCrop model was used for simulation research. The AquaCrop model was calibrated and validated using measured data for 2022 and 2023. The simulation results showed that the simulated values of soil water content, canopy coverage and yield were in good agreement with the observed values. The performance index (EF) of the model is 0.70 to 0.94, indicating that the overall performance of the model is high. Specifically, the root mean square error (RMSE) of soil water content ranged from 2.04 to 3.42%, the RMSE of canopy coverage ranged from 8.27 to 9.54%, and the RMSE of yield ranged from 0.28 to 0.33 tons / ha. In addition, the coefficient of determination (R^2) is between 0.85 and 0.94, which further verifies the high fitting degree and reliability of the model. The total water requirement of forage oats during the whole growth period was 230.7–333.1 mm, and the total water consumption was 214.7–315.4 mm. The drainage loss is 1.2–10.6 mm, accounting for 0.3%–5.40% of the total water demand. In 2022 and 2023, the water productivity (WP) of the second crop is 0.1–0.4 kg / m³ higher than that of the first crop. These findings help to provide valuable insights for optimizing agricultural water management practices in the region.

Keywords Shallow-buried drip irrigation, Water balance analysis, Water productivity, Soil water dynamics, Forage oats grown twice annually

Agriculture and animal husbandry lay the foundation of national stability by ensuring food security. China's annual demand for high-quality forage reaches 120 million tons, and more than 2 million tons of high-quality forage such as alfalfa and oat grass are imported annually. The annual gap is more than 50 million tons, and the market demand is huge¹. The irrigation area along the Yellow River in Inner Mongolia is not only the main grain producing area, but also an important forage base. Forage oats belong to gramineae, with high nutritional quality, salt tolerance, drought resistance, cold tolerance, wide adaptability and high yield^{2,3}. In order to alleviate the shortage of forage grass, the oat planting pattern in this area was changed from one season a year to two seasons a year. The system change has led to the unclear growth process and water consumption law of oats, the contradiction between supply and demand of regional water resources has intensified, the utilization efficiency of farmland irrigation water has declined, and the bottleneck of water resources has threatened the sustainable development of agriculture and animal husbandry^{4,5}. Therefore, exploring the growth and development and water consumption process of drip-irrigated oats in the Yellow River irrigation area of Inner Mongolia is the core of scientific planning and management of irrigation systems and the key link to achieve water conservation⁶.

¹Institute of Water Resources and Hydropower Research, Yinshanbeilu Grassland Eco-Hydrology National Observation and Research Station, Beijing 100038, China. ²Institute of Water Resources for Pastoral Area Ministry of Water Resources, Hohhot 010020, China. ³College of Water Conservancy and Civil Engineering, Inner Mongolia Agricultural University, Hohhot 010018, China. ✉email: nmxubing@163.com; imau_wgs@163.com

With the iteration of agricultural water-saving technology^{4–8} Hydrological models^{9,10} have shown irreplaceable value in the study of crop water consumption and the impact of water resources management¹¹.

Extensive experimental and numerical studies have been conducted to understand water consumption in irrigation regions^{12–14}. However, experimental approaches are often costly, time-intensive, and constrained by site-specific outcomes. Models such as AquaCrop^{15–17} HYDRUS^{18–21} Soil and Water Assessment Tool (SWAT)²² and Soil-Water-Atmosphere-Plant (SWAP)²³ are effective in analyzing soil water migration, transformation, and consumption processes within these systems. For instance, Liang et al.²⁴ employed the HYDRUS-1D model to simulate water and salt migration in wasteland soils, demonstrating that intense evaporation drives this migration, thereby validating the model's accuracy in simulating vertical water and salt movement. Ruimin et al.²⁵ utilized the SWAT-DynamicParam model to effectively characterize time-varying parameters, emphasizing the importance of capturing dynamic hydrological processes. Similarly, Yuan et al.²³ applied the SWAP model to simulate the water and salt balance in sunflower cultivation in the Hetao region, highlighting the frequent interactions between soil water and groundwater. Their findings demonstrated that sunflowers can efficiently utilize groundwater to meet their growth demands. Post-harvest irrigation to manage soil salinity is essential for ensuring the normal growth of sunflowers in subsequent years.

While hydrological models have been successfully applied to simulate comprehensive water consumption processes, crop-specific parameters—such as canopy cover and root depth—are often oversimplified or treated as static, failing to capture their continuous and dynamic changes²⁵. To address these limitations, researchers have developed coupled models that integrate hydrological and crop growth processes for more accurate simulations of water consumption in irrigation regions. For example, Hao et al.²⁶ developed a distributed model based on the one-dimensional agricultural hydrological HYDRUS-EPIC framework, which analyzed soil water, salt, and crop growth under existing irrigation practices. Their findings highlighted high soil salinity as a major constraint on crop yields. Wang et al.²⁷ created a distributed water transformation model that couples irrigation and drainage processes with soil water movement and crop growth, enabling a detailed quantitative characterization of the supply-consumption-drainage dynamics within irrigation systems. Similarly, Wang et al.²⁸ employed a HYDRUS-1D and EPIC coupling model to simulate soil water and salt dynamics as well as crop growth for winter wheat at the Fengqiu National Key Agricultural Ecological Experimental Station. Their study demonstrated that salt stress reduced evapotranspiration, primarily by diminishing crop transpiration, and that saline-alkali stress adversely impacted grain yield.

Although these coupled models have improved the understanding of water consumption processes in agricultural systems, their added complexity can present challenges. To address these issues, the AquaCrop model was developed as a water-driven crop hydrological model that simulates crop productivity under both soil moisture and rain-fed conditions using meteorological data²⁹. WANG et al.³⁰ AquaCrop was used to analyze the yield change and soil water balance of summer maize in the piedmont of North China Plain, and the growth and water consumption process of maize were characterized. Zhu et al.³¹ utilized AquaCrop to study the effects of soil water and salinity on winter wheat growth under saline-fresh irrigation schemes, providing optimized irrigation strategies. Their results validated AquaCrop's capability to effectively simulate soil water and salinity dynamics, biomass, and grain yield for winter wheat. M et al.³² further demonstrated AquaCrop's utility in predicting the impacts of soil, water, nutrients, and climate on biomass, yield, and water use efficiency across various crops. While elucidating the water consumption process in the agricultural environment, they emphasized its effectiveness in simulating rice growth and yield under different water conditions. Although these advances have been made, there are few studies on the water consumption process of forage oats under double cropping patterns and shallow drip irrigation techniques in arid and semi-arid areas, which fills the gap of existing research, and also verifies the applicability of AquaCrop under double cropping patterns and shallow drip irrigation techniques in this area.

In this study, the AquaCrop model was used to simulate and verify the water consumption process of forage oats in arid and semi-arid areas under the double cropping mode and shallow buried drip irrigation technology. By calibrating and validating the model, the growth and water consumption processes of forage oats were simulated, and the water balance and irrigation water consumption processes were evaluated. The study solved the challenges brought by the practice of shifting from single-season planting to double-season planting and limited irrigation, and provided important insights for improving the irrigation water use efficiency of the forage production system and optimizing the allocation of agricultural water resources in the Yellow River irrigation area of Inner Mongolia.

Materials and methods

Overview of the study area

The Yellow River Basin in Inner Mongolia, located at the northernmost section of the Yellow River (37°35'–41°50'N, 106°10'–112°50'E), has a total conventional water resource availability of 5.145 billion m³, with per capita water resources estimated at 856 m³, leading to a rigid water deficit of 1.816 billion m³. The cultivated land area spans 46.18 million acre, accounting for 27.31% of the total cultivated land in the region, with approximately 9 million acre classified as saline-alkali land, representing about 23% of the cultivated area. Annual precipitation ranges from 250 to 300 mm, with primary crops including corn, wheat, oats, alfalfa, and sunflowers. The study area is situated in the Tumd Left Banner of Hohhot (40°38'–40°44'N, 111°16'–111°24'E), characterized by gentle terrain and a continental monsoon climate. The total area of the study site is 2,560 acre, of which oats occupy 472 acre, with an average annual precipitation of 318.9 mm. Most precipitation occurs during the summer months from June to August, with 257.8 mm (80.91% of annual rainfall) falling during the oat growth period (April 6 to October 8 or October 14). The average temperature during this period is 18.93 °C, with a maximum daily temperature of 28.7 °C occurring in June and July, and a minimum daily temperature of 2.6 °C recorded in April. The average annual evaporation is 1,870.3 mm, with 2,876.5 h of sunshine and total annual solar radiation of

133.82 kcal.cm⁻². The frost-free period is relatively short, lasting about 133 days. The soil in the top 0-40 cm is primarily sandy loam, while soil below 40 cm is predominantly sandy. Oats are irrigated using a subsurface drip irrigation method. The location of the test site and groundwater observation well is shown in Fig. 1. (The satellite image is from <https://www.91weitu.com/default.htm>).

Experimental design and data acquisition

Field experiments were conducted in the demonstration area of Tumd Left Banner, Hohhot, Inner Mongolia, from April to October in 2022 and 2023. The planting area of oats is 40 hm² and the irrigation method is shallow drip irrigation. The first crop variety used was Baylor 2, followed by Meida for the second crop. The subsurface drip irrigation system employed had a belt spacing of 45 cm, with oat row spacing of 12 cm and plant spacing ranging from 3 cm to 5 cm. Each drip irrigation belt managed an average of four oat rows, with a subsurface installation depth of 8 cm. For AquaCrop model management, field conditions indicated no runoff, a weed coverage rate of 5%, and no plastic film mulching. The experimental data collected in 2022 and 2023 were used as the simulated values of AquaCrop model, and the soil water content, canopy coverage and yield of the model were calibrated and verified by trial and error method. Five-point sampling method was used for sampling detection, and each point was sampled three times. The soil water content, canopy coverage and other indicators were monitored once a week, and the yield was measured at harvest. Soil water content was measured by drying method, and crop height was measured by tape method. The yield was evaluated by collecting 1 m² samples from each plot, drying at 105 °C for 30 min, then drying to constant weight at 75 °C, and then multiplying the dry weight by the planting density to calculate the yield. Canopy coverage was determined by leaf area index, and the extinction coefficient was 0.71^{36,37}. Before the experiment, the soil texture of each monitoring point was determined by Wilkes method soil particle grading (Table 1). The depths of sampling layers were 0–10 cm, 10–20 cm, 20–40 cm, 40–60 cm, 60–80 cm, 80–100 cm and 100–120 cm, respectively. A groundwater level observation well was established in the test field and monitored once a week. Meteorological data include rainfall, radiation, temperature, wind speed, humidity, etc. The data is from the automatic weather station in the experimental area (HOBO-U30, Onset Computer Corp., Bourne, MA, USA). The growth process of oats is shown in Fig. 2.

(1) Soil physical properties in the study area.

Soil samples were collected from seven layers in the experimental site. The sampling depths were 0–10 cm, 10–20 cm, 20–40 cm, 40–60 cm, 60–80 cm, 80–100 cm, and 100–120 cm respectively. Three samples were taken from each layer. The undisturbed soil samples were soaked and saturated by Wilcox method³⁵ and then placed

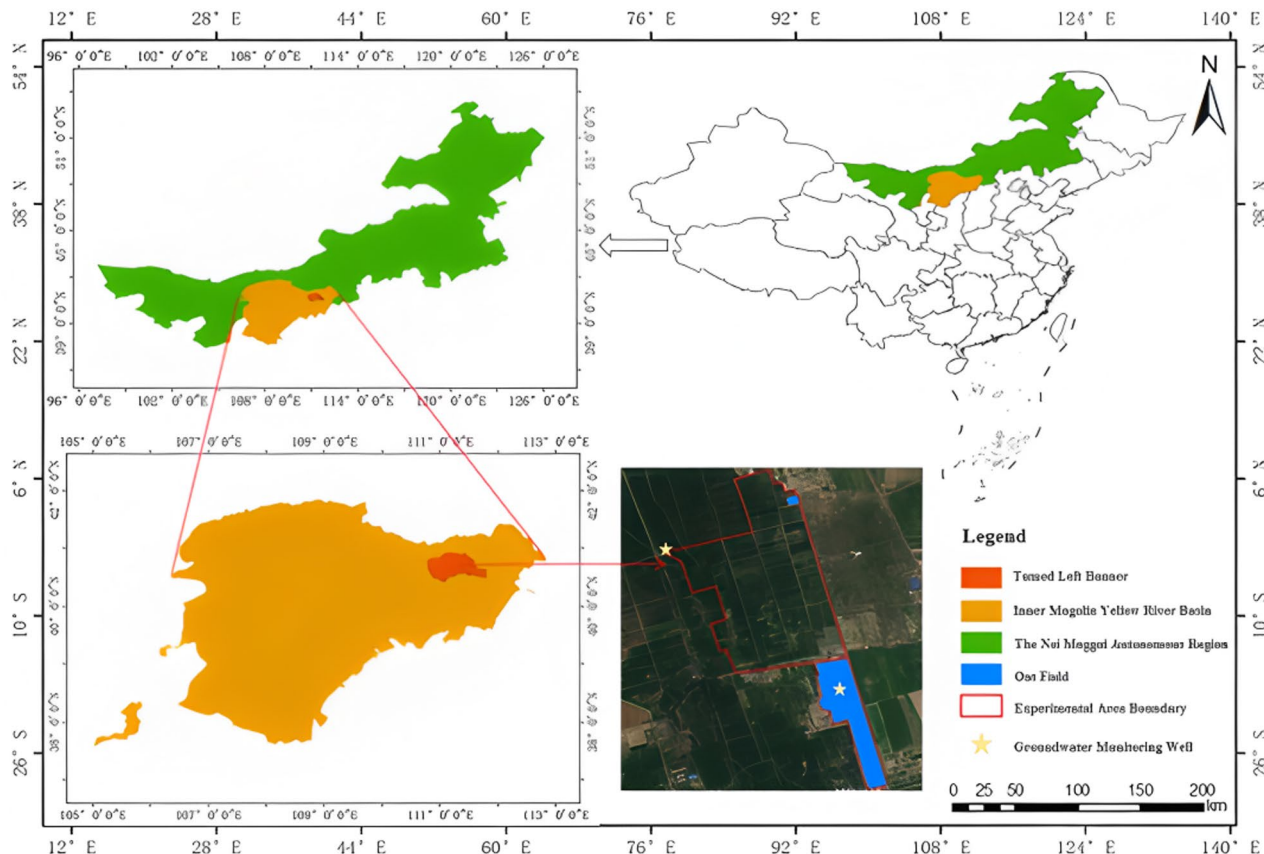


Fig. 1. Test site and groundwater observation well location.

Soil Depth/(cm)	Particle distribution/%			Soil bulk density /(gcm^{-3})	Field capacity /(%)	$\theta_s/(\text{cm}^3 \times \text{cm}^{-3})$	$\theta_r/(\text{cm}^3 \times \text{cm}^{-3})$	Soil type
	Clay (<0.002 mm)	Silt (0.05~0.002 mm)	Sand (5~0.05 mm)					
0~10	12.58	32.14	55.28	1.44	36.8	41.0	0.15	Sandy Loam
10~20	14.25	26.58	59.17	1.46	36.2	40.5	0.16	Sandy Loam
20~40	13.37	36.29	50.34	1.40	35.1	37.6	0.16	Sandy Loam
40~60	6.52	2.63	90.85	1.56	29.2	36.5	0.09	Sandy Soil
60~80	6.43	2.75	90.82	1.56	29.2	36.5	0.09	Sandy Soil
80~100	6.79	2.67	90.54	1.56	29.2	36.5	0.09	Sand Soil
100~120	6.37	2.77	90.86	1.56	29.2	36.5	0.09	Sandy Soil

Table 1. Soil physical characteristics of 0 ~ 120 cm. Note: θ_s : Percentage of saturated water content. θ_r : wilting coefficient.

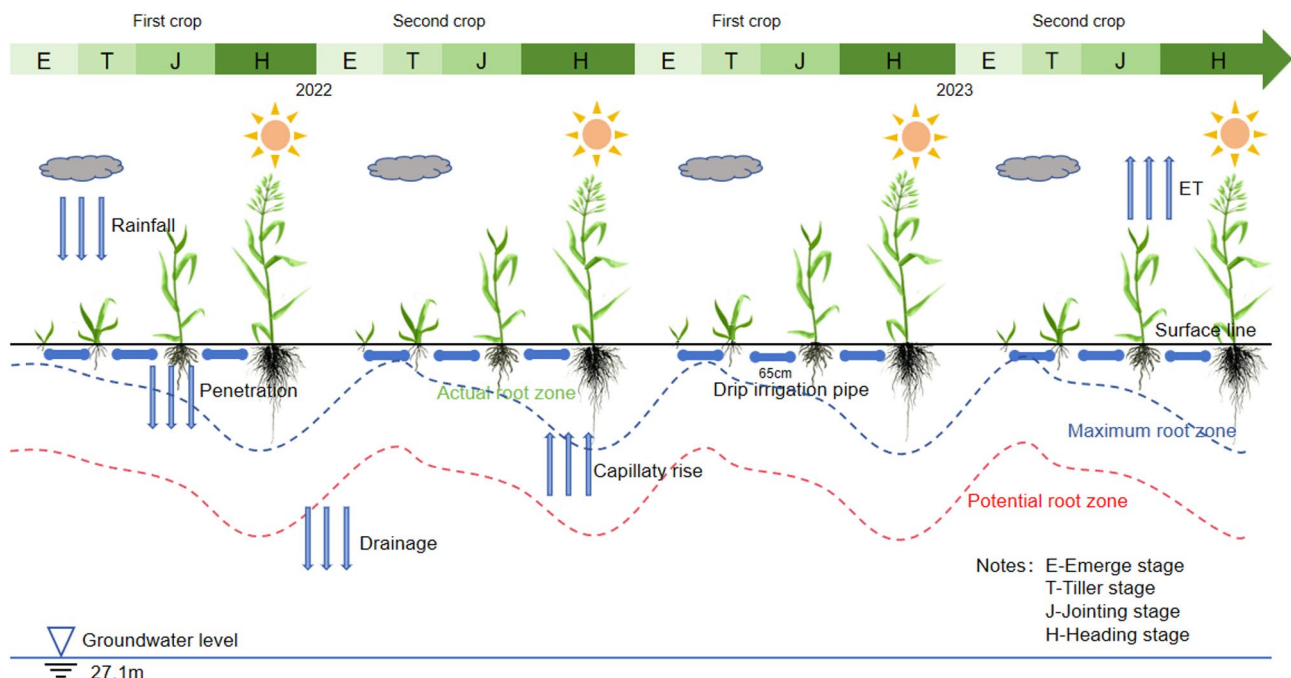


Fig. 2. Sketch of oat growth process.

on the air dried soil. The gravity water in the soil samples was discharged under the action of the suction of the air dried soil. After a period of time, the soil field capacity, saturated water content and soil bulk density could be determined, and the soil particle size gradation at each point was determined by dry particle size analyzer. The sand, silt, and clay content for each soil layer at each sampling point is summarized in Table 1.

(2) Crop growth period.

Oat forage is cultivated in two seasons annually. In 2022, the first season was planted on April 6 and harvested on July 9. The second season was planted on July 22 and harvested on October 8. For 2023, the first crop was planted on April 5 and harvested on July 8, followed by the second crop, which was planted on July 25 and harvested on October 14. The statistics of oat growth period are shown in Table 2.

(3) Irrigation practice.

According to the local actual situation, the irrigation times, irrigation time and irrigation amount in 2022 and 2023 were counted. When the soil water content reached 50% of the total soil available water, irrigation was carried out. In 2022, the first crop only received three irrigations, with irrigation quotas of 25 mm, 30 mm and 30 mm, respectively, and the total irrigation quota was 85 mm. In 2022, the second crop will be irrigated 6 times, each irrigation quota is 30 mm, and a total of 180 mm will be irrigated. In 2023, the first crop was irrigated seven times, and the irrigation quota was 30, 30, 40, 40, 40, 40 mm, a total of 260 mm. In 2023, the second crop also received seven irrigations, with quotas of 15, 30, 30, 30 and 30 mm, respectively, for a total of 195 mm. Therefore, the total irrigation amount of the two crops was 230 mm in 2022 and 455 mm in 2023. The irrigation schedule for 2022 and 2023 is shown in Table 3.

(4) Groundwater depth.

Year	Crops	Implantation time	Harvest time	Growth phase				Total days (d)
				Emerge / (d)	Tiller / (d)	Jointing / (d)	Heading / (d)	
2022	First Crop	6 April	9 July	3	28	44	20	95
	Second Crop	22 July	8 October	4	22	36	17	79
2023	First Crop	5 April	8 July	4	26	43	22	95
	Second Crop	25 July	14 October	3	23	38	18	82

Table 2. The crop growth period table of two crops of Oats in 2022 and 2023.

Year	Crops	Irrigation time	Irrigation requirement/(mm)	Rain fall /(mm)	Evapotranspiration /(mm)
2022	First Crop	5 April	25	140.2	165.3
		5 June	30	14.8	28.9
		11 June	30		
		30 June	30	29.4	60.4
	Second Crop	11 August	30	9.3	63.79
		28 August	30	1.9	39.08
		7 September	30	1.5	26.57
		14 September	30		
		27 September	30	0.5	44.57
2023	First Crop	6 April	30	6.71	42.7
		20 April	30	17.73	51.4
		4 May	40	0.9	27.6
		10 May	40	1.16	39.8
		22 May	40	7.55	43.6
		2 June	40		
		14 June	40	1.9	45.7
	Second Crop	14 August	15	30.78	61.3
		23 August	30	0.58	45
		31 August	30	23.73	54.8
		11 September	30	14.1	43.8
		19 September	30	3.37	25.2
		25 September	30		
		3 October	30	2.58	37.6

Table 3. Irrigation schedule in 2022 and 2023.

The test site primarily contains deep groundwater, with an average annual depth ranging from 25 to 29 m. The average groundwater depth during the growth periods in 2022 was 27.9 and 27.6 m, while in 2023 it was 25.7 and 27.5 m. The months of June, July, and August represent peak irrigation periods, during which groundwater levels exhibit significant fluctuations. After crop harvest, water consumption decreases, leading to a subsequent rise in groundwater levels. The data indicate that, with the implementation of water-saving measures in recent years, groundwater depth has gradually increased. Given that the groundwater depth exceeds 3 m, its impact on this study is minimal³⁶. The data come from national monitoring wells. The change of groundwater depth is shown in Fig. 3.

Aquacrop model simulation

(1) The basic principle of AquaCrop model.

The AquaCrop model is a universal crop growth simulation tool developed by the Food and Agriculture Organization (FAO) to reflect the response of crop biomass and yield to water availability. It evaluates food security and assesses the environmental and management impacts on crop production. The model strikes an effective balance between simplicity, accuracy, and stability, utilizing fewer parameters, and is widely employed in designing deficit irrigation strategies. The theoretical foundation of the model is based on the yield-water response relationship expressed as³⁷, according to Eq. 1.

$$\left(1 - \frac{Y}{Y_x}\right) = K_y \left(1 - \frac{ET}{ET_x}\right) \quad (1)$$

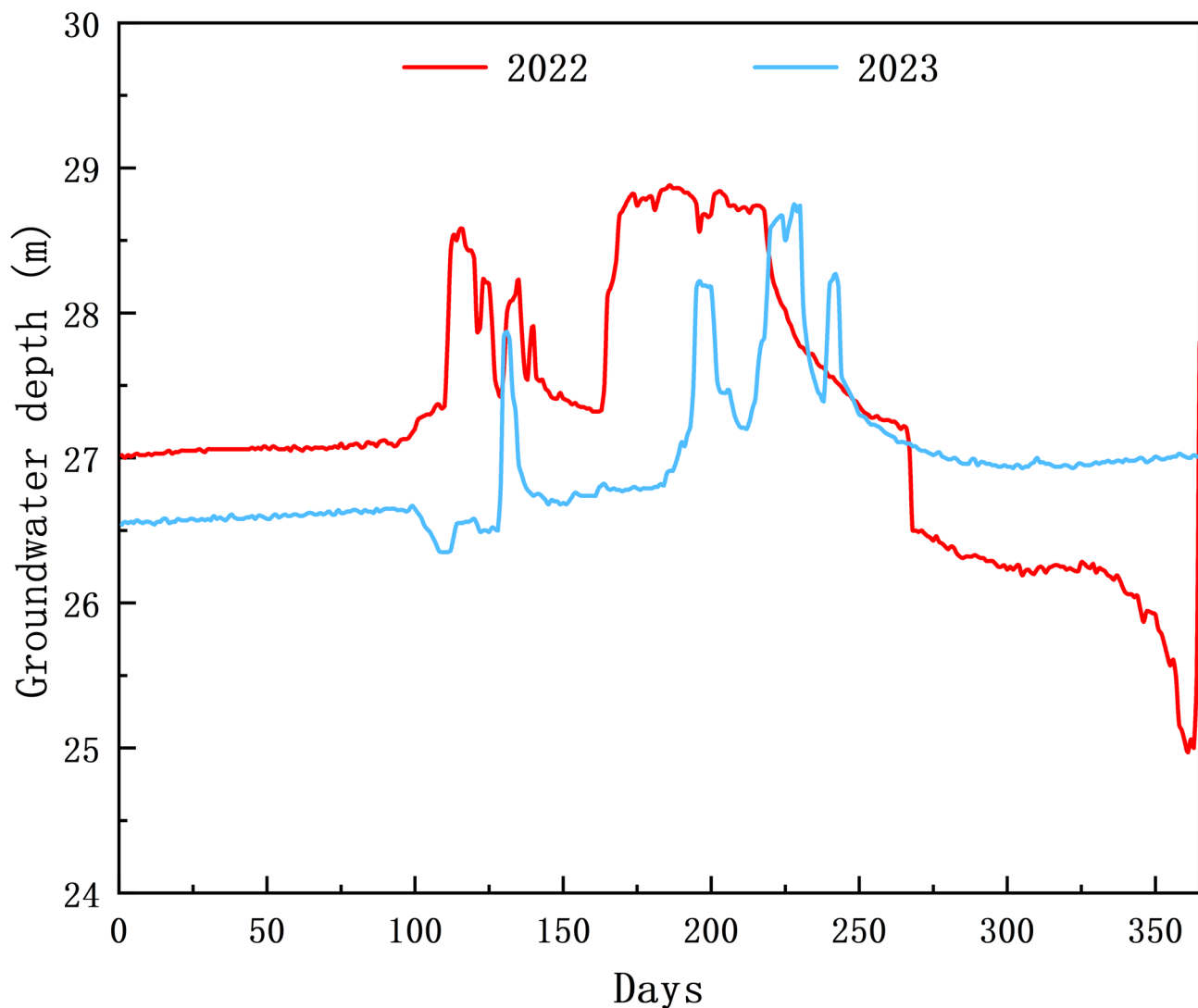


Fig. 3. Groundwater level changes in 2022 and 2023.

Y_x and Y are the maximum and actual yield, $\text{kg} \times \text{hm}^{-2}$; K , the proportionality factor between relative yield decline and relative reduction in evapotranspiration; ET_x and ET the maximum and actual evapotranspiration. Through further refinement, the equations for calculating crop transpiration, aboveground biomass, and yield are as follows³⁸, according to Eqs. 2–4.

$$T_r = K_s \times (K_{CTr,x} \times CC^*) \times ET_o \quad (2)$$

$$B = 100 \times K_{sb} \times WP^* \times \sum \frac{T_r}{ET_o} \quad (3)$$

$$Y = B \times HI \quad (4)$$

T_r represents crop transpiration, mm; K_s represents soil water stress coefficient, %; $K_{CTr,x}$ represents all the different factors that distinguish the actual crop from the reference crop, %; CC^* represents the calibrated canopy coverage, %; B denotes biomass, $\text{t} \times \text{hm}^{-2}$; K_{sb} represents the low temperature stress coefficient, %; WP^* denotes standardized water production efficiency, $\text{kg} \times \text{m}^{-2}$; HI represents crop harvest index, %; Y represents the final crop yield, $\text{t} \times \text{hm}^{-2}$.

REW (Readily Evaporable Water) is derived from the field capacity (FC) of the soil surface layer and the soil water content of the permanent wilting point (PWP) (5) :

$$0 \leq \text{REW} = 10 \left(FC - \frac{PWP}{2} \right) Z_{e,surf} \leq \quad (5)$$

FC volume water content at field capacity vol%; PWP volume water content at permanent wilting point vol%; $Z_{e, \text{surf}}$ thickness of the evaporating soil surface layer in direct contact with the atmosphere 0.040 m.

Total Available Soil Water (TAW) is the amount of water that can be contained in the fine soil portion of the considered soil volume between field capacity and permanent wilting point (6):

$$\text{TAW} = 1000 (\theta_{\text{FC}} - \theta_{\text{WP}}) Z \left(1 - \frac{\text{Vol\%}_{\text{gravel}}}{100} \right) \quad (6)$$

TAW total available soil water in the considered soil volume, mm; θ_{FC} volumetric water content at field capacity, $\text{m}^3 \times \text{m}^{-3}$; θ_{WP} water content at permanent wilting point, $\text{m}^3 \times \text{m}^{-3}$; Z depth of the considered soil volume, m; $\text{Vol\%}_{\text{gravel}}$ volume percentage of the gravel fraction in the soil volume.

(2) Model simulation unit division.

The simulated profile depth of the oat field was set to 120 cm. According to the measured soil texture (Table 1), the profile was divided into 7 layers, and observation points were set at 10,20,40,60,80,100 and 120 cm, respectively. The simulation timeline for the oat field is as follows: April 6 to July 9 for the first crop of 2022, July 22 to October 8 for the second crop, April 5 to July 8 for the first crop of 2023, and July 25 to October 14 for the second crop. The simulation durations for these periods are 95 days, 79, 95 and 82 days, respectively. The initial time step for the model is set to one day.

(3) Weather variables.

The meteorological data required for the study were from an automatic weather station located in the experimental area (HOBO-U30, Onset Computer Corp., Bourne, MA, USA). Figure 4 (2022a and 2023b) illustrate the temperature and rainfall statistics for 2022 and 2023. The annual rainfall for 2022 was 316.9 mm, while in 2023 it was 320.81 mm. Temperature ranges during these years varied from -20.9 to 37 °C in 2022 and -27 to 34.41 °C in 2023. The average temperatures for 2022 and 2023 were -14.9 to 28.4 °C and -21.5 to 28.4 °C, respectively. During the growth periods (April 6 to October 8 in 2022 and April 5 to October 14 in 2023), rainfall totaled 298.8 and 194.9 mm, 94.29 and 60.75% of the annual rainfall, respectively. The average temperatures during these growth periods were 19.19 °C for 2022 and 18.66 °C for 2023. The daily average maximum temperatures were 29.4 and 28.0 °C, observed in June and July, while the daily average minimum temperatures were 3.7 and 2.6 °C, recorded in April. Crop evapotranspiration (ET_0) was calculated using the Penman-Monteith equation.

(4) Crop parameters.

Crop parameter files are mainly composed of crop development, ET, crop production and soil water stress, soil salinity stress, air temperature stress and so on. The crop growth parameters such as Maximum canopy coverage (CC_x), number of plants per hectare, Initial canopy coverage (CC_0) and Maximum effective root depth (Z_{max}) were obtained by field observation. The base temperature and upper temperature limit are recommended for C3 crops by the model. Reference Harvest Index (HI_0), Canopy growth coefficient (CGC), Canopy attenuation coefficient (CDC), Standard water productivity (WP^*), Crop coefficient when canopy is complete but prior to senescence ($K_{\text{Cr}, x}$) and Water stress parameters ($P_{\text{exp, upper}}, P_{\text{exp, lower}}, P_{\text{sto, upper}}, P_{\text{sen, upper}}$) were determined based on the reference parameters provided by the model, and the trial and error method⁴³ was used to correct them.

Water Productivity(WP).

In this paper, Water Productivity (WP) were calculated by using oat yield in 2022 and 2023⁴³.

The water productivity (WP) of each irrigation system was calculated using Eq. 7.

$$\text{WP} = \frac{Y}{ET} \quad (7)$$

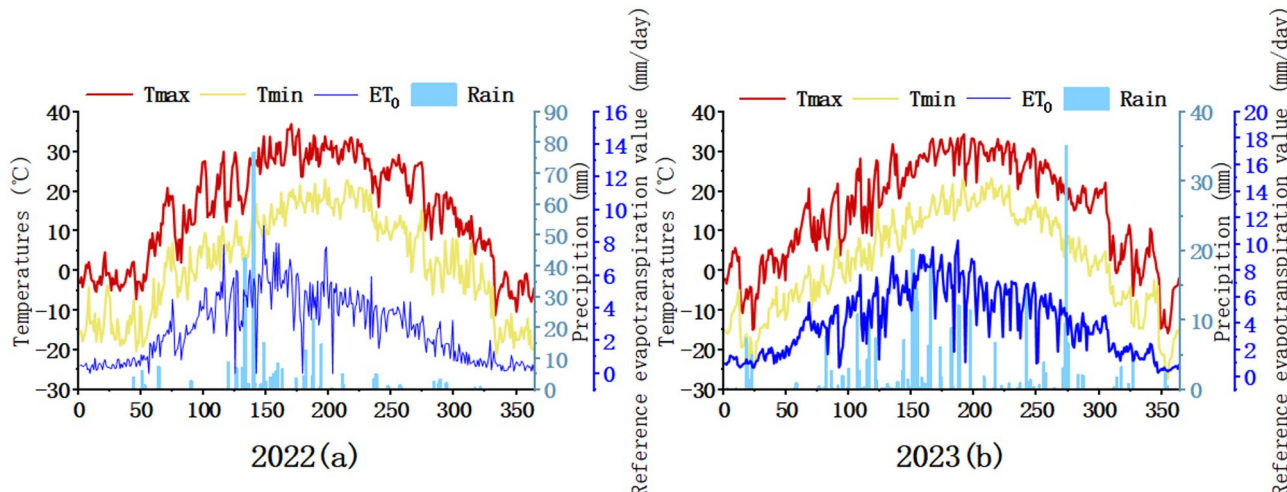


Fig. 4. Chart of meteorological changes in 2022 and 2023.

WP is water productivity $\text{kg} \times \text{m}^{-3}$; Y is yield $\text{kg} \times \text{da}^{-1}$; and ET is Water requirement during growth period mm. Model calibration verification.

In this study, soil moisture content, leaf area index, and yield data from 2022 were employed to calibrate the model parameters, while data from 2023 were used to verify the simulation accuracy. The model calibration and validation processes utilized metrics such as root mean square error (RMSE), model performance index (EF), coefficient of determination (R^2)⁴⁰. The flow chart of calibration and verification is shown in Fig. 5 according to Eqs. 8–10.

$$\text{RMSE} = \sqrt{\frac{\sum_{i=1}^n (M_i - S_i)^2}{n}} \quad (8)$$

$$\text{EF} = \frac{\sum_{i=1}^n (M_i - \bar{M})^2 - \sum_{i=1}^n (M_i - S_i)^2}{\sum_{i=1}^n (M_i - \bar{M})^2} \quad (9)$$

$$R^2 = \left[\frac{\sum_{i=1}^n (M_i - \bar{M})(S_i - \bar{S})}{\left[\sum_{i=1}^n (M_i - \bar{M})^2 \right]^{0.5} \left[\sum_{i=1}^n (S_i - \bar{S})^2 \right]^{0.5}} \right]^2 \quad (10)$$

n is the number of samples; M_i and S_i are the measured values and simulated values of the parameters, respectively; \bar{M} is the measured average value; RMSE is used to describe the error of the model estimation, and the smaller the value, the better; EF and R^2 are used to describe the relative error of the model, and the value is 0~1. The closer the simulated value is to 1, the smaller the deviation between the simulated and measured values, indicating a higher degree of accuracy in the model simulation.

Results

Model calibration

The model was calibrated using measured soil moisture data from 2022. The simulated soil moisture values aligned closely with the observed values, effectively reflecting the dynamic changes in soil moisture. As shown in Table 4, the calibration accuracy for soil water content across the two oat seasons was $\text{RMSE} \leq 4$, with $0.7 \leq \text{EF} \leq 0.9$ and $R^2 \geq 0.85$. These findings confirm that the simulated soil moisture values were consistent with the measured data. Research demonstrates that the AquaCrop model accurately captures the fundamental changes in soil moisture dynamics.

The model calibration also included canopy coverage and yield data from 2022. The results indicated that the simulated values for both canopy coverage and yield were in good agreement with the measured data, effectively representing the dynamic changes in crop indices. According to Table 5, the calibration accuracy for canopy coverage (CC_w) and yield for oats across the two seasons yielded $\text{RMSE} \leq 9$, $0.85 \leq \text{EF} \leq 0.95$, $0.95 \geq R^2 \geq 0.85$.

In this experiment, the measured data of field experiment in 2022 was used to calibrate the model parameters, and the measured data of field experiment in 2023 was used to verify the model. In this study, two brands of Oats

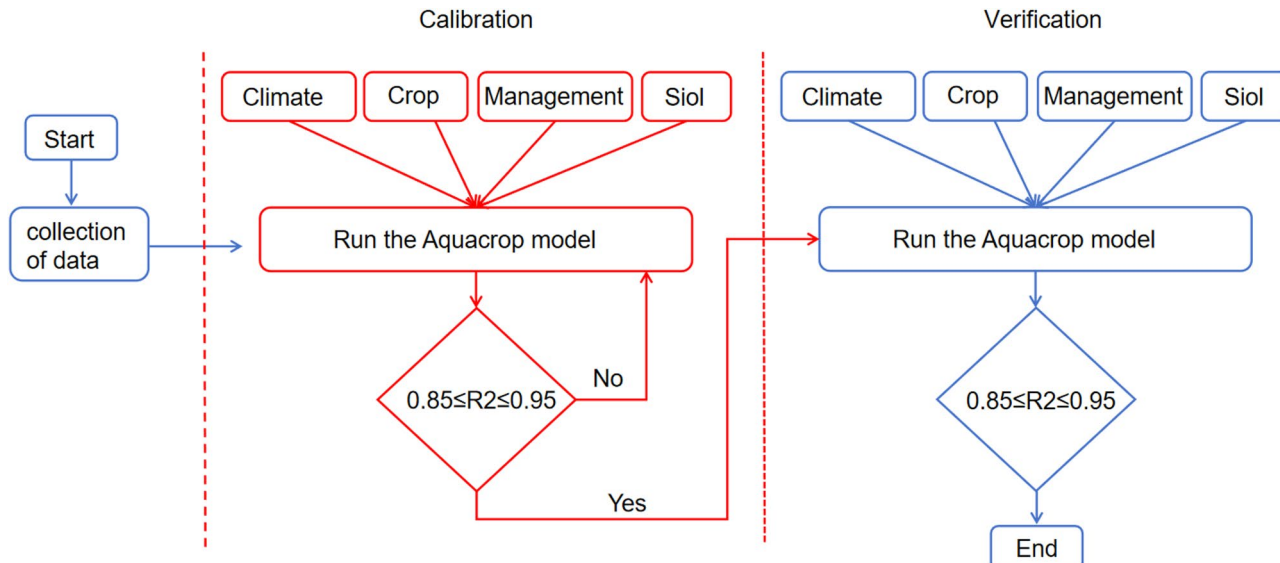


Fig. 5. Calibration, verification flow chart.

Year	Test Treatment	Soil Depth/(cm)	RMSE(%)	EF	R ²
2022 (Model calibration)	First crop	0~10	2.66	0.82	0.85
		10~20	2.78	0.83	0.85
		20~40	2.86	0.84	0.86
		40~60	2.20	0.82	0.86
		60~80	2.43	0.85	0.87
		80~120	2.65	0.83	0.89
	Second crop	0~10	3.42	0.76	0.87
		10~20	2.76	0.81	0.85
		20~40	2.78	0.83	0.85
		40~60	2.78	0.70	0.85
		60~80	2.84	0.79	0.86
		80~100	2.95	0.81	0.87

Table 4. Evaluation of accuracy indicators for soil water content..

Year	Test Treatment	Statistical Index	RMSE	EF	R ²
2022 (Model calibration)	First crop	CC _w /(%)	8.53	0.87	0.93
		Yield/(ton·ha ⁻¹)	0.33	0.90	0.92
	Second crop	CC _w /(%)	8.27	0.94	0.94
		Yield/(ton·ha ⁻¹)	0.29	0.91	0.92

Table 5. Evaluation of accuracy indicators for CC_w and yield of Oats.

Parameter	Description	Nominal value	Unit
HI ₀	Reference Harvest Index	43	
CGC	Canopy growth coefficient	0.105	%·d ⁻¹
CDC	Canopy attenuation coefficient	0.079	%·d ⁻¹
CC _x	Maximum canopy coverage	87	%
WP*	Standard water productivity	16.5	g·m ⁻²
T _{base}	Base temperature	3	°C
T _{upper}	Upper limit temperature	45	°C
K _{cfr,x}	Crop coefficient when canopy is complete but prior to senescence	1.10	-
CC _o	Initial canopy coverage	0.68	%
P _{exp,upper}	Upper limit of effect of water stress on canopy	0.12	
P _{exp,lower}	Lower limit of influence of water stress on canopy	0.54	
P _{sto,upper}	Upper limit of water stress on stomatal conductance	0.55	
P _{sen,upper}	Upper limit of effect of water stress on early canopy senescence	0.90	
Z _{max}	Maximum effective root depth	1.15	m
Z _{min}	Minimum effective root depth	0.1	m
	Number of plants per hectare	2,778,723	Plants·hm ²

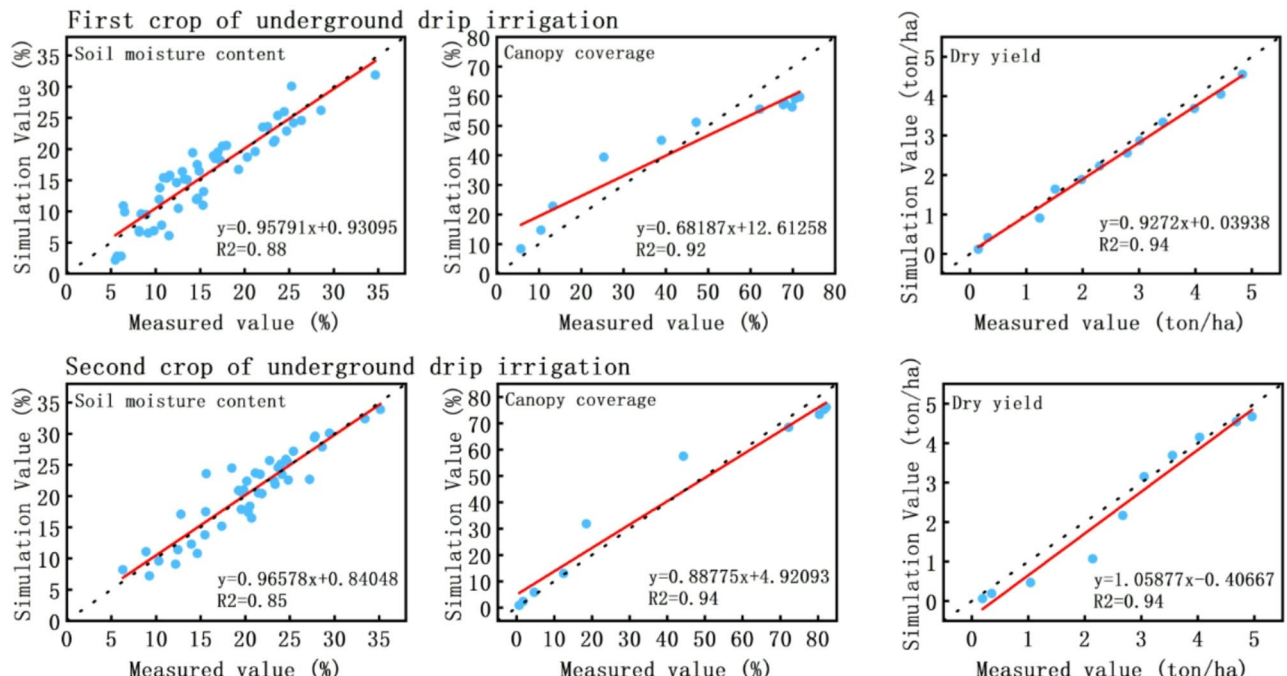
Table 6. AquaCrop model first crop Oats (Baylor 2) parameter list.

were selected, of which Baylor 2 Oats had a longer growth period of 90 ~ 100 days and a higher yield of 3500 ~ 6000 kg·hm⁻². Because forage Oats are planted twice a year, the remaining planting period is short, so the second crop is selected by meida. The growth period is generally 75–85 days, and the yield is relatively stable at 4500–5500 kg·hm⁻². Due to different varieties and different genes, the growth period and physiological performance are different, so the crop parameters are also relatively changed. Most of the parameter values are similar, but there are also different parameter values (such as canopy growth coefficient, maximum effective root depth, etc.) that affect the results. The main crop parameters of aquacrop model^{41,42} are shown in Tables 6 and Table 7.

Model validation

The model was validated using the measured soil moisture, canopy coverage, and yield data from 2023, with all parameters set to the values obtained during model calibration. The verification results are illustrated in Fig. 6. The evaluation indices for soil moisture are as follows: RMSE was 3.17, EF was 0.76, and R² was 0.88 for the first season; for the second season, RMSE was 2.47, EF was 0.83, and R² was 0.85. The evaluation indices for canopy

Parameter	Description	Taking Values	Unit
HI_0	Reference Harvest Index	45	
CGC	Canopy growth coefficient	0.154	$\% \times d^{-1}$
CDC	Canopy attenuation coefficient	0.041	$\% \times d^{-1}$
CC_x	Maximum canopy coverage	89	%
WP*	Standard water productivity	17	$g \cdot m^{-2}$
T_{base}	Base temperature	3	°C
T_{upper}	Upper limit temperature	45	°C
$K_{cTr, x}$	Crop coefficient when canopy is complete but prior to senescence	1.10	-
CC_o	Initial canopy coverage	0.66	%
$P_{exp, upper}$	Upper limit of effect of water stress on canopy	0.11	
$P_{exp, lower}$	Lower limit of influence of water stress on canopy	0.55	
$P_{sto, upper}$	Upper limit of water stress on stomatal conductance	0.56	
$P_{sen, upper}$	Upper limit of effect of water stress on early canopy senescence	0.91	
Z_{max}	Maximum effective root depth	0.95	m
Z_{min}	Minimum effective root depth	0.1	m
	Number of plants per hectare	2,769,231	Plants.hm ²

Table 7. AquaCrop model second crop Oats (Meida) parameter list.**Fig. 6.** Verification diagram of soil moisture content, canopy cover, and yield for the year 2023. Note: Blue dots denote the scatter plot comparing simulated versus observed values, while the red line represents the fitted regression line.

coverage were: RMSE of 9.54, EF of 0.85, and R^2 of 0.92 for the first season; for the second season, RMSE was 9.03, EF was 0.93, and R^2 was 0.94. For yield, the evaluation indices were as follows: RMSE of 0.30, EF of 0.90, and R^2 of 0.94 for the first season; and for the second season, RMSE was 0.28, EF was 0.94, and R^2 was 0.91. As shown in Fig. 5, the accuracy of the parameters meets the requirements and closely aligns with the calibration results. These findings indicate that the AquaCrop model effectively captures the fundamental dynamics of crop growth and development.

Soil moisture dynamic analysis process

The dynamic changes of soil moisture in oats were analyzed by using the simulation results of AquaCrop model in 2022 and 2023. The detailed soil moisture changes are shown in Fig. 7. In 2022, the soil moisture dynamics during the first crop growth period showed that the irrigation amount was small and the rainfall was large,

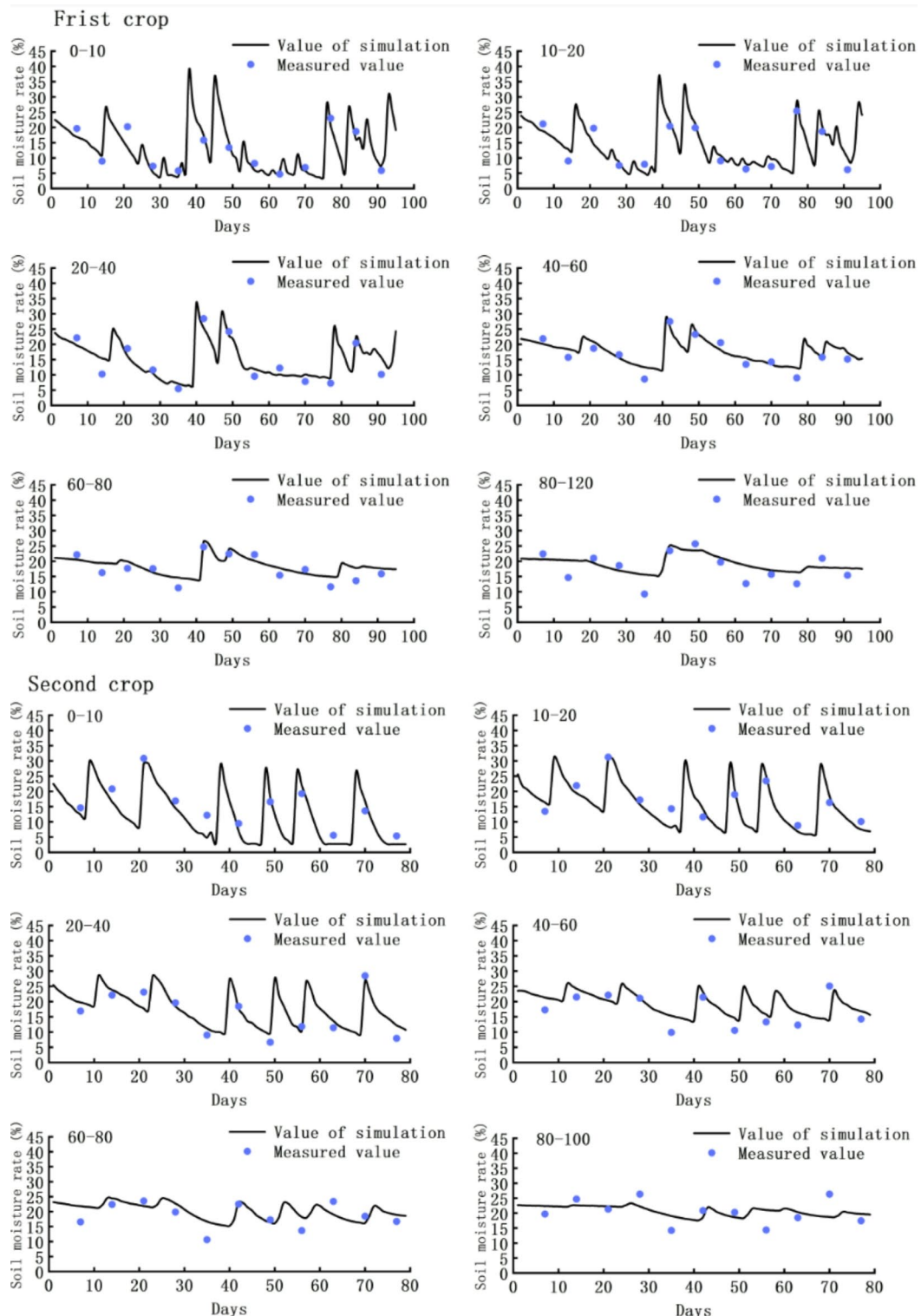


Fig. 7. The change process of soil moisture content in the experimental site in 2022.

accounting for 78.3% of the annual precipitation. On the 40th day of growth, the maximum daily rainfall reached 76.9 mm, and the soil water content reached the peak of 38.5, 36.2, 33.2, 28.7, 26.4% and 23.9% in 10, 20, 40, 60, 80 and 120 cm soil layers, respectively. Due to frequent rainfall, surface soil moisture exhibited considerable fluctuations, while deeper soil layers retained moisture more effectively, resulting in slower consumption and minimal fluctuation. During the growth period of the second crop, rainfall was sparse, totaling only 19.7 mm throughout the entire growth period. Consequently, fluctuations in surface soil moisture were minimal, and the

moisture content in deeper layers remained relatively stable. Notably, soil moisture decreased rapidly from the 40th to the 60th day during the second crop growth period.

The changes in soil moisture for oats in 2023 are presented in Fig. 8. According to local irrigation observations, the test site was irrigated seven times in 2023, with the last irrigation occurring on July 10. Throughout the growth period in 2023, rainfall accounted for 60.75% of the total annual precipitation, with the first and second stubbles contributing 22.44 and 38.31%, respectively. Consequently, the soil moisture of the second stubble exhibited greater variability compared to the first stubble. The average soil water content for each layer in the second crop

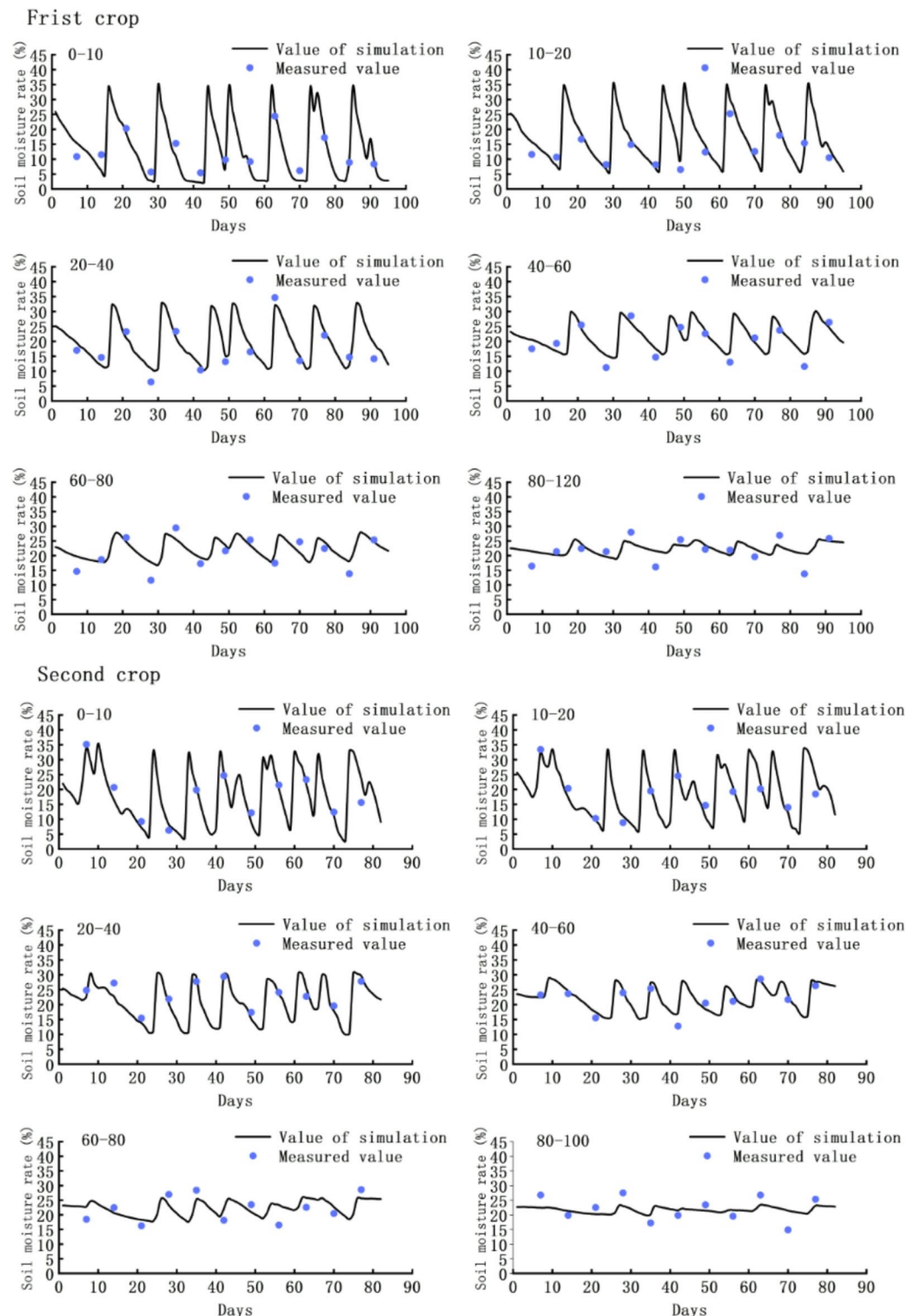


Fig. 8. The change process of soil moisture content in the experimental site in 2023.

was 0.24, 0.25, 0.22, and 0.21 $\text{cm}^3 \cdot \text{cm}^{-3}$, respectively. Before and after the first irrigation, the increases in soil moisture content for the 10, 20, 40, 60, 80 and 100 cm layers were 87.82, 89.58, 69.47, 47.85, 31.87 and 17.56%, respectively. In 2022, changes in soil moisture for oats were primarily influenced by rainfall, while in 2023, irrigation had a more significant impact, resulting in notable differences in soil moisture dynamics between the two years.

The change process of crop physiological index

(1) Canopy coverage effect.

Figure 9 presents the canopy coverage index for oats in 2023. The canopy coverage index exhibited significant variation corresponding to the growth stages of the crops, with growth patterns in both years following a similar trend of gradual increase, culminating in a single peak. In 2022, the first crop experienced a rapid increase in canopy coverage from the 15th to the 45th day. However, due to low soil moisture from the 45th to the 71st day, the increase slowed. Following irrigation on the 71st day, the growth rate of the canopy coverage index accelerated once more. The second crop in 2022 also grew rapidly from the 30th to the 49th day, but then growth decelerated after the 49th day, ultimately achieving a canopy coverage index of 81% by the end of the growth period. In 2023, the growth curve for the first crop's canopy coverage index was relatively smooth, with fewer fluctuations. The second crop experienced a rapid increase in the canopy coverage index from the 20th to the 45th day, followed by a slowdown in growth thereafter. Notably, when the canopy coverage index increased rapidly, there was a significant decrease in soil moisture content. Conversely, when the canopy coverage index increased slowly, the decrease in soil moisture was less pronounced, suggesting that a more rapid increase in the canopy coverage index correlates with greater water demand.

The maximum canopy coverage index for the two crops in 2022 was 85 and 79%, respectively. This difference can be attributed to the concentrated rainfall during the growth period of the first crop, resulting in a higher canopy coverage index compared to the second crop. In 2023, the maximum canopy coverage index for the two

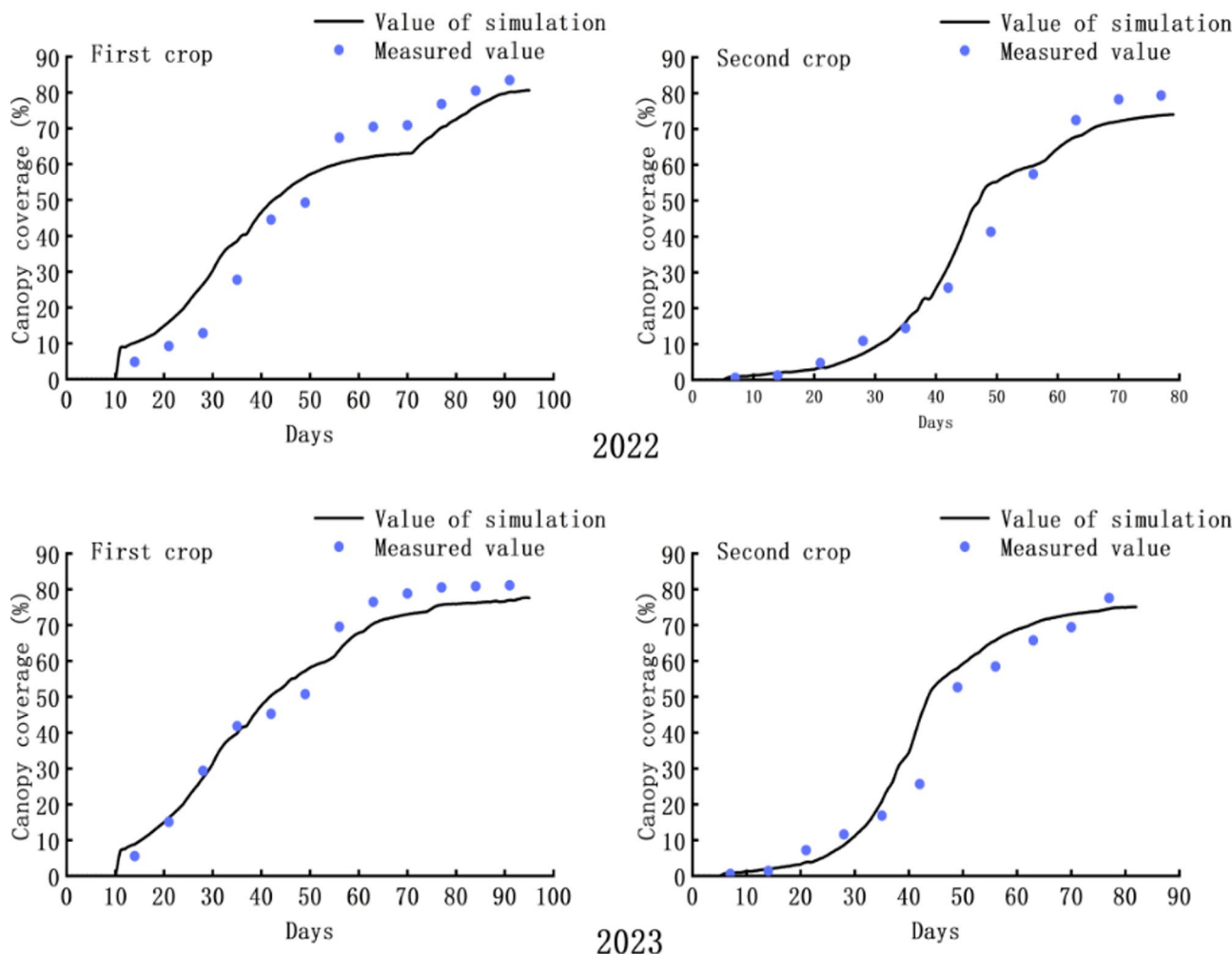


Fig. 9. Comparison of simulated and measured values of canopy coverage index of experimental land in 2022 and 2023.

Years	Crop number	Yield/(kg·hm ⁻²)	Years	Crop number	Yield/(kg·hm ⁻²)
2022	First crop	5132	2023	First crop	4835
	Second crop	4324		Second crop	4964

Table 8. Canopy coverage and yield index of forage Oats in 2022 and 2023.

Crop number	Times	Basic parameter	Numerical
First crop	4/6~7/9	R/(mm)	248.1
		I/(mm)	85
		△W/(mm)	-13.5
		ET/(mm)	309
		E/(mm)	83.9
		T/(mm)	225.1
Second crop	7/22~10/8	P/(mm)	8.9
		R/(mm)	50.7
		I/(mm)	180
		△W/(mm)	-7.1
		ET/(mm)	214.7
		E/(mm)	54.3
		T/(mm)	160.4
		P/(mm)	8.9

Table 9. Water balance of soil profile of different crops in 2022. Note: R: Rain fall; I: Irrigation capacity; DW: The difference between the initial soil water content and the initial soil water content; ET: evapotranspiration; E: Evaporation; T: Transpiration; P: Percolation.

crops was 81 and 82%, respectively, indicating minimal difference due to similar rainfall and irrigation quotas for both crops.

(2) Characterization of yield change of oats in two stubbles per year.

Oat yields increased progressively with plant growth. In 2022, the rainfall was predominantly concentrated during the growth period of the first crop, which, combined with a longer growth duration, resulted in a yield of 808 kg·hm⁻² higher than that of the second crop. In 2023, rainfall was more evenly distributed during the growth period of the second crop, leading to a yield increase of 129 kg·hm⁻² compared to the first crop. The average yield growth rate throughout the entire growth period was approximately 50.89 to 60.54 kg·hm⁻² per day. Notably, the growth rate for the second crop in both 2022 and 2023 was faster than that of the first crop, with rates ranging from 0.71 to 9.64 kg·hm⁻² respectively. The evaluation table of canopy coverage and oat yield accuracy index is shown in Table 8.

Water balance analysis

Based on the principle of water balance, the water balance of soil moisture during the growth period was estimated by using the data of 2022 and 2023. The results are presented in Tables 9 and 10. In 2022, the evapotranspiration for the first and second crops of oats was 309 and 214.7 mm, respectively, with total drainage recorded at 10.6 and 8.9 mm. In 2023, evapotranspiration for the first and second crops was 315.4 and 304.2 mm, respectively, with total drainage at 1.2 and 2.6 mm. Overall water consumption during the growth period accounted for 93.39 to 95.69% of the total introduced water (rainfall plus irrigation), while drainage accounted for 0.36 to 5.40% of the introduced water. In 2022, soil evaporation for the first and second stubbles constituted 27.14 and 25.30% of total evapotranspiration, respectively, while plant transpiration represented 72.86 and 74.70%, respectively. In 2023, soil evaporation for the first and second crops accounted for 18.58 and 23.54% of total evapotranspiration, corresponding to 17.65 to 22.52% of the introduced water. Plant transpiration accounted for 81.42 and 76.46% of total evapotranspiration, comprising 73.17 to 77.34% of the introduced water. Because the canopy coverage of the second crops in 2022 and 2023 was greater than that of the first crops, transpiration for the second crops was higher. Total evapotranspiration for both crops in 2023 exceeded that of both crops in 2022 by 95.5 mm. The amount of drainage during the growth periods in 2022 and 2023 ranged from 1.2 to 10.6 mm, representing 0.36 to 5.40% of the total introduced water. Notably, the total drainage for both crops in 2023 was 15.7 mm less than that for both crops in 2022.

Analysis of water productivity

Based on the simulation results of oat yield in 2022 and 2023, the relationship between crop yield and water productivity (WP) was analyzed by using WP. The calculation results are summarized in Tables 11 and 12. The WP for the first and second crops of oats in 2022 were 1.61 and 2.01 kg × m⁻³, respectively, while in 2023, these values were 1.53 and 1.63 kg × m⁻³, respectively. The WP for the first and second stubbles decreased by 0.08

Crop number	Times	Basic parameter	Numerical
First crop	4/5~7/8	R/(mm)	72
		I/(mm)	260
		△W/(mm)	-15.4
		ET/(mm)	315.4
		E/(mm)	58.6
		T/(mm)	256.8
		P/(mm)	1.2
Second crop	7/25~10/14	R/(mm)	122.9
		I/(mm)	195
		△W/(mm)	-11.1
		ET/(mm)	304.2
		E/(mm)	71.6
		T/(mm)	232.6
		P/(mm)	2.6

Table 10. Water balance of soil profile of different crops in 2023. Note: R: Rain fall; I: Irrigation capacity; DW: The difference between the initial soil water content and the initial soil water content; ET: evapotranspiration; E: Evaporation; T: Transpiration; P: Percolation.

Basic parameter	Times	Crop number	Numerical
I/(mm)	4/6~7/9	First crop	85
	7/22~10/8	Second crop	180
ET/(mm)	4/6~7/9	First crop	309
	7/22~10/8	Second crop	214.7
Y/(kg·hm ⁻²)	4/6~7/9	First crop	5132
	7/22~10/8	Second crop	4324
Ya/(kg·hm ⁻²)	4/6~7/9	First crop	4237
	7/22~10/8	Second crop	2537
WP/(kg·m ⁻³)	4/6~7/9	First crop	1.61
	7/22~10/8	Second crop	2.01

Table 11. Water productivity of oats in 2022. Note: I: Irrigation capacity; ET: evapotranspiration; Y: Crop yield; Ya: Unirrigated crop yield; WP: Water productivity.

Basic parameter	Times	Crop number	Numerical
I/(mm)	4/5~7/8	First crop	260
	7/25~10/14	Second crop	195
ET/(mm)	4/5~7/8	First crop	315.4
	7/25~10/14	Second crop	304.2
Y/(kg·hm ⁻²)	4/5~7/8	First crop	4835
	7/25~10/14	Second crop	4964
Ya/(kg·hm ⁻²)	4/5~7/8	First crop	2925
	7/25~10/14	Second crop	3108
WP/(kg·m ⁻³)	4/5~7/8	First crop	1.53
	7/25~10/14	Second crop	1.63

Table 12. Water productivity of oats in 2023. Note: I: Irrigation capacity; ET: evapotranspiration; Y: Crop yield; Ya: Unirrigated crop yield; WP: Water productivity.

and $0.38 \text{ kg} \times \text{m}^{-3}$, respectively. This decrease may be attributed to higher evapotranspiration in 2023 compared to 2022, resulting in a slight reduction in unit water output.

Discussion

In this study, field experiments and numerical simulations were conducted in the demonstration area of Tumed Left Banner, Hohhot, Inner Mongolia, from 2022 to 2023. A comprehensive database encompassing

meteorological, soil, crop, and irrigation factors was established, and the AquaCrop model was utilized for simulation research. The model underwent calibration and validation using data from 2022 to 2023, including soil water content, canopy coverage, and crop yield. After calibration and validation, the simulated values generated by the AquaCrop model exhibited good agreement with the observed values, effectively simulating the growth and water consumption processes of forage oat under the double-season planting mode.

Zhou Qilong et al.⁴³ reported that the hay yield of oat Beile 2 in Tibet reached 9,082 kg·hm⁻², while the yield for oat Meida was approximately 6,900 kg·hm⁻². In contrast, this study observed hay yields for oat Beile 2 ranging from 4,835 to 5,132 kg·hm⁻², and for oat Meida, yields varied between 432 and 4,964 kg·hm⁻². The lower yields in this study can be attributed to the two-season planting model and the shorter growth period of forage oats. Additionally, environmental conditions and regional differences in oat cultivation contribute to the observed yield reductions. Ma et al.⁴⁴ noted that with a planting row spacing of 15 cm, the hay yield was 4,300 kg·hm⁻², which is slightly lower than the yields observed in this study. This difference may stem from the narrower planting row spacing of 12 cm and variations in planting density in this research. Despite the lower yields, Ma's study reported a water productivity of 2.55 kg·m⁻², which is higher than that observed in this research. Shah et al.⁴⁵ found that the fresh weight of oats was between 12 411.6 kg · hm⁻² and 16 572.85 kg·hm⁻². The experimental area of Shah has a humid subtropical climate, characterized by an average annual rainfall of 790 mm, which may have caused waterlogging and eventually led to lower yields than in this study. Cheng et al.⁴⁶ examined the impact of climate change on forage oat yields in northern Shanxi and concluded that climatic conditions were the primary factors influencing yields, with soil parameters having minimal significance. The climatic conditions and yield (fresh weight: 14,006–17,786 kg·hm⁻²) of the yield area in this study were consistent with the results of this research. Zhao et al.⁴⁷ cultivated oats in a rainproof pond, reporting hay yields between 4,395.55 and 12,960.64 kg·hm⁻², significantly higher than those recorded in this study. This underscores the influence of climatic conditions on oat growth and development.

The study identified water consumption for oats during the two seasons of 2022 and 2023 as follows: 309.2, 147.7, 315.4, and 304.2 mm, respectively. The average water consumption rates were calculated at 3.25, 2.72, 3.32, and 3.71 mm·d⁻¹. Xu Bing et al.⁴⁸ conducted field experiments in Lhasa, determining that the water demand for oats throughout the entire growth period was 570 mm, with water consumption varying between 464 and 570 mm under different conditions. Utilizing the Hydrus model, Wang et al.⁴⁹ found that total water consumption for oats ranged from 404 to 571 mm. The discrepancies in water consumption observed in this study can be attributed to significant regional variations and different planting methodologies, such as single versus double growing seasons. Wang et al.⁵⁰ reported findings from the ecotone between agriculture and animal husbandry at the northern foot of the Yinshan Mountain in Wuchuan County, Inner Mongolia, where water consumption of oats aligned closely with this study's results. However, fluctuations in soil moisture from 0 cm to 40 cm in this study were greater than those reported elsewhere, particularly between the 40 cm and 60 cm depths. The water productivity (WP) for oats in Ma et al.⁵¹ study ranged from 3.41 to 3.86 kg·m⁻³, exceeding the WP observed in this research by 1.4 to 2.33 kg·m⁻³, possibly due to the application of nitrogen fertilizer, which enhanced water productivity.

This study provides valuable insights into the growth and water use patterns of drip-irrigated oats cultivated in two seasons per year. The findings serve as a reference for enhancing irrigation water use efficiency in forage production systems and optimizing the allocation of agricultural water resources in irrigated regions.

Conclusions

This study utilized the AquaCrop model to simulate the growth and water consumption processes of oats, identifying the patterns of water use throughout the entire growth cycle across two seasonal plantings. The key conclusions are summarized as follows:

The AquaCrop model has a high fitting accuracy between the simulated value and the observed data, indicating that it has high reliability in simulating the growth and water consumption process of oats. The dynamic change trend of canopy coverage of oats in the two years was similar, which showed the stable simulation ability of the model to this index in different years. Although the yield of the first crop was higher than that of the second crop in both years, the change of water productivity (WP) was significantly different. The WP of the first crop in 2022 and 2023 was lower than that of the second crop, which may be related to the water use efficiency of different seasons. The total water consumption during the growth cycle ranged from 214.7 to 315.4 mm, accounting for 93.39 % to 95.69 % of the total water input (rainfall plus irrigation), indicating a high dependence of oat growth on water. The drainage loss is the smallest, accounting for only 0.36 % to 5.40 % of the total water delivery, indicating that there is room for optimization in water management. In each growth stage, the soil water content decreased the fastest and the water consumption was the largest at the jointing stage, which emphasized the importance of water management at this stage.

This study explored the growth process and water consumption process of drip-irrigated oats in two seasons in one year. The experimental scale was limited to the small-scale water consumption process of farmland, and there was a lack of comparison of variables such as different drip irrigation belt spacing, buried depth and irrigation quota. According to the needs of relevant policies, this experiment will reset the comparison of different variables in the future, and combine the conditions on the regional scale to quantitatively evaluate the growth process and water consumption process of drip-irrigated oats in the irrigation area along the Yellow River in Inner Mongolia in one year and two seasons, so as to provide an effective basis for the implementation of relevant policies.

Data availability

The data are contained within the article.

Received: 13 February 2025; Accepted: 14 August 2025

Published online: 01 October 2025

References

- Hou, Y., Wang, H., Li, J., Li, C. & Chen, F. Research progress on the effects of intercropping of gramineae and leguminous forage crops on forage quality and nitrogen uptake. *Crops* 1–11, (2025).
- Tang, J. et al. Large-scale protein extraction from oat hulls using two hydrodynamic cavitation techniques: A comparison of extraction efficiency and protein nutritional properties. *Food Chem.* 471142724–142724 (2025).
- Ye, X. et al. Advances and perspectives in forage oat breeding. *Acta Geogr. Sin.* 32(02), 160–177 (2023).
- Kishor, N. et al. Soil water distribution and water productivity in red cabbage crop using superabsorbent polymeric hydrogels under different drip irrigation regimes[J]. *Agric. Water Manage.* 295, 108759 (2024).
- Rajput, J. et al. Water accounting of groundwater over exploited districts in Haryana and Punjab States to analyse impacts of water conservation measures on water availability[J]. *Water Supply.* 24 (9), 3093–3117 (2024).
- Rajput, J. et al. Development of single and dual crop coefficients for drip-irrigated broccoli using weighing type field lysimeters in semi-arid environment[J]. *Environ. Dev. Sustain.*, 1–27 (2024).
- Rajput, J., Choudhary, R. & Kothari, M. Optimization of cropping patterns in the Bhimsagar Canal irrigation scheme using linear programming approach[J]. *Water Pract. Technol.* 20(1), 15–34 (2025).
- Bisht, H. et al. Impacts of climate change on phenology, yield, and water productivity of wheat in a semi-arid region of India using the CERES-Wheat model[J]. *J. Water Clim. Change* 15(10), 5089–5106 (2024).
- Yang, S. T. et al. *model. Acta Geogr. Sin.* 78, 1691–1702 (2023).
- Beven, K. How to make advances in hydrological modelling. *Hydrolog. Res.* 50, 1481–1494 (2019).
- Pei, Y. S., Xu, J. J., Xiao, W. H., Yang, M. Z. & Hou, B. D. Development and application of the water amount, quality and efficiency regulation model based on dualistic water cycle. *J. Hydraul Eng.* 51, 1473–1485 (2020).
- Wang, Y. Evaluation of Farmland Water Circulation Health in Irrigated Area of North China Plain: A Case Study of Junliu Irrigated Area. Master's Thesis, Hebei University of Engineering, Handan, China, (2021).
- Zhang, M. & Thesis Study on law of hydrological cycle and water resources regulation in Jinghui Canal Irrigation District. Ph.D. Chang-an University, Xi-an, China (2021).
- Rong, W. et al. Long-term responses of the water cycle to climate variability and human activities in a large arid irrigation district with shallow groundwater: insights from agro-hydrological modeling. *J. Hydrol.* 626, (2023).
- Meng, J. H., Wang, Y. N., Lin, Z. X. & Fang, H. T. *Perspective Crop Growth Models Nongye Jixie Xuebao* 55, 1–15 (2024).
- Li, N., Li, Y., Yang, Q., Asim & Dong, H. Z. Simulating climate change impacts on cotton using aquacrop model in China. *Agr Syst* 216103897– (2024).
- Rogy, N., Pastor, A., Sferratore, A., Géheniau, N. & Hélias, A. Loiseau taking the spatio-temporal effects of climate change into account for life cycle assessment of prospective scenarios to secure water supplies in agricultural areas. *Sci. total Environ.* 915169345– (2024).
- Gao, Z. G., Zhong, R. L., Yang, S., Li, X. G. & Yang, X. Y. *Recent. Progresses Res. Appl. Hydrus Model. China Soils* 54, 219–231 (2022).
- Su, K., Mu, L., Zhou, T. & Yang, H. M. Quantifying Spatiotemporal transfer of soil water and salt between intercrop root zones under alfalfa/spring wheat strip intercropping based on HYDRUS-2D. *Agr. Ecosyst. Environ.* 375109172–109172 (2024).
- Swain, S. S. et al. Modelling and optimization of Urea super granule (USG) placement depth in paddy cultivation under check basin irrigation using HYDRUS-2D model[J]. *Soil Tillage. Res.* 241, 106104 (2024).
- Li, Y. Lanzhou Study on maize yield estimation using remote sensing technology integrated with coupled WOFOST and HYDRUS models[D]. Ph.D. Thesis, University, Lanzhou, China (2012).
- Li, B. G. et al. Freeze-Thaw cycle altered the simulations of groundwater dynamics in a heavily irrigated basin in the temperate region of China. *Water Resour. Res.* 60, e2023WR036151–e2023WR036151 (2024).
- Yuan, C. F. & Feng, S. Y. Simulation of soil water-salt flux of sunflower farmland in Hetao irrigation district based on SWAP model. *J. Water Resour. Water Eng.* 34, 19–27+36 (2023).
- Li, L., Shi, H. B., Jia, J. F. & Liu, H. Y. Simulation of water and salt transport of uncultivated land in Hetao irrigation district in inner Mongolia. *Nongye Jixie Xuebao* 26, 31–35 (2010).
- Liu, R. et al. Time-varying parameters of the hydrological simulation model under a changing environment. *J. Hydrol.* 643, 131943 (2024).
- Hao, Y. et al. Distributed modeling of soil water-salt dynamics and crop yields based on HYDRUS-EPIC model in Hetao Irrigation District. *Trans. Chin. Soc. Agric. Eng.* 31 (11), 110–116 (2015).
- Wang, P., Lu, Z. & Huo, Z. L. Distributed water transformation model based on multi-process coupling in rice irrigation area. *J. Hydraul Eng.* 52, 1163–1173 (2021).
- Wang, X. et al. Evaluating the effects of irrigation water salinity on water movement, crop yield and water use efficiency by means of a coupled hydrologic/crop growth model. *Agric. Water Manage.* 185 13–26 (2017).
- Wang, L. X., Wu, J. S., Li, Q., Guo, J. Y. & Xue, H. X. A review on the research and application of aqua crop model. *ADV. ATMOS. SCI.* 30, 1100–1106 (2015).
- Wang, J., Huang, F. & Li, B. Quantitative analysis of yield and soil water balance for summer maize on the Piedmont of the North China plain using aquacrop. *Front. Agric. Sci. Eng.* 2, 295–310 (2015).
- Zhu, C. L. et al. Simulation and evaluation of cycle irrigation with brackish and fresh water for winter wheat based on aquacrop model. *Nongye Jixie Xuebao* 53, 330–342 (2022).
- Maniruzzaman, M., Talukder, M. S. U., Khan, M. H., Biswas, J. C. & Nemes, A. Validation of the aquacrop model for irrigated rice production under varied water regimes in Bangladesh[J]. *Agric. Water Manage.* 159, 331–340 (2015).
- Wei, X. & Nie, Z. Sensitivity analysis and optimization of leaf area index related parameters of dryland wheat based on APSIM model[J]. *Chin. J. Eco-Agric.* 32 (1), 119–129 (2024).
- Liu, J. D., Yu, Q. & Liu, C. M. Agrometeorological numerical simulation of canopy extinction coefficient of winter wheat in Huang-Huai-Hai plain. *Chin. J. Eco-Agric.* 03, 51–54 (2002).
- Xie, X. Q. & Wang, L. J. Observation and Analysis of Water Environmental Elements. CSB 7–9 (1998).
- Xue, X., Cai, J. B., Yu, Y. D., Zhang, B. Z. & Han, Y. A. Quantifying groundwater contributions and threshold in the growth stages for winter wheat. *CAE* 40(20), 101–111 (2024).
- Steduto, P., Hsiao, T. C., Raes, D. & Fereres, E. AquaCrop—The FAO crop model to simulate yield response to water: I. Concepts and underlying principles. *Agron. J.* 101, 426–437 (2009).
- Ren, X. H., Wang, H. X., Liu, C. M. & Fan, L. Water-saving potential analysis of spring wheat in Altay based on aquacrop model. *Chin. J. Eco-Agric* 30, 1638–1648 (2022).
- Fernández, J. E., Alcon, F., Diaz-Espejo, A., Hernandez-Santana, V. & Cuevas, M. V. Water use indicators and economic analysis for on-farm irrigation decision: A case study of a super high density Olive tree orchard. *Agric. Water Manag.* 237, 106074–106074 (2020).
- Sun, S. J., Zhang, L. L., Chen, Z. J. & Sun, J. *Adv. AquaCrop Model. Res. Application Sci. Agric. Sin.* 50, 3286–3299 (2017).
- Li, J. et al. Study on the Simulation of the CanopyGrowth of Spring Wheat in the Northeast Based on the AquaCrop Model. *ISWCR* 20, 106–110 (2013).

42. Zhou, Y. X., Wang, Q. J., Zhang, J. H., Tan, S. & He, B. Simulation analysis of the impact of climate change on the yield of winter wheat in Shaanxi Province based on the aquacrop model. *ISWCR* **25**, 357–364 (2018).
43. Zhou, Q. L., Duoji, D. Z., Liu, Y. F., Yang, W. C. & Liao, Y. C. Analysis of yield stability and adaptability of forage oat hay based on AMMI model. *Seed* **39**, 79–82 (2020).
44. Ma, Q., You, Y., Shen, Y. & Wang, Z. K. Adjusting sowing window to mitigate climate warming effects on forage oats production on the Tibetan Plateau[J]. *Agric. Water Manage.* **293**, 108712 (2024).
45. Shah, J. et al. A.Optical-sensor-based nitrogen management in oat for yield enhancement. *Sustainability-Basel* **13**, 6955 (2021).
46. Cheng, H. Q., Hou, Q. Q., Zhu, M. & Yang, X. Effects of climate change and crop rotation system on forage Oats yield in Northern Shanxi Province. *Zuo Wu Xue Bao* **50**, 2599–2613 (2024).
47. Zhao, B. P. et al. Effect of limited irrigation on yield and water use efficiency of oats. *Agric. Res. Arid Areas* (01), 105-108+115 (2007).
48. Xu, B. et al. Research on optimal irrigation schedule of Oats by CROPWAT in Lhasa of Tibet. *Agric. Res. Arid Areas* **33**, 35–39 (2015) (183).
49. Wang, G. et al. Study on water and heat transport of different types of vegetations and fields in Pengbo alpine irrigation district of Qinghai. *Tibet Plateau J. Hydrol.* **618**, 129201 (2023).
50. Ma, Q., Zhang, X., Wu, Y., Yang, H. M. & Wang, Z. K. Optimizing water and nitrogen strategies to improve forage oat yield and quality on the Tibetan plateau using APSIM. *Agronomy* **12**, 933 (2022).
51. Wang, G. et al. Exploring the water-Soil-Crop dynamic process and water use efficiency of typical irrigation units in the Agro-Pastoral ecotone of Northern China. *Plants* **13**, 1916–1916 (2024).

Author contributions

Conceptualization, G.W. X.M. and Y.C.; methodology, D.T. G.W. and Y.C.; software, L.X. and J.Z.; validation, B.X. J.Z. and X.M.; formal analysis, G.W. and D.T.; investigation, X.L.; resources, B.X. G.W. and D.T.; data curation, Y.C. L.X. and J.Z.; writing—original draft preparation, Y.C. and G.W.; writing—review and editing, X.L. and D.T.; visualization, J.Z. and X.M.; supervision, B.X.; project administration, Y.C. and L. X.; funding acquisition, B.X. and D.T.; Y.C. and G.W. is the first author of this article. B.X. and G.W. is the communication author of this article. All authors have read and agreed to the published version of the manuscript.

Funding

This study was, in part, supported by the key technology research and demonstration of efficient water-saving in the forage area of the Yellow River Basin in Inner Mongolia, (grant No.2023JBGS0014), Study on the establishment and application of the integrated model of drip irrigation technology for precise decision-making of silage maize in Tumochuan Plain (grant No.2023YFHH0080) and Study on the water consumption characteristics and soil environmental regulation mechanism of alfalfa with different growth years in the Yellow River region of Inner Mongolia (grant No.MKGP2024JK015). Research and integrated demonstration of key technologies for seedling preservation, rain storage, supplementary irrigation and steam reduction in dryland agriculture in eastern Mongolia, Grant No. 2023YFDZ0075. Technical Demonstration of Collaborative Utilization of Water-Soil-Plant Resources System in Ecological Agriculture and Animal Husbandry Area, Grant No. 2021CG0012. Key Projects of DaMaoQi Irrigation Experimental Station.

Declarations

Competing interests

The authors declare no competing interests.

Additional information

Correspondence and requests for materials should be addressed to B.X. or G.W.

Reprints and permissions information is available at www.nature.com/reprints.

Publisher's note Springer Nature remains neutral with regard to jurisdictional claims in published maps and institutional affiliations.

Open Access This article is licensed under a Creative Commons Attribution-NonCommercial-NoDerivatives 4.0 International License, which permits any non-commercial use, sharing, distribution and reproduction in any medium or format, as long as you give appropriate credit to the original author(s) and the source, provide a link to the Creative Commons licence, and indicate if you modified the licensed material. You do not have permission under this licence to share adapted material derived from this article or parts of it. The images or other third party material in this article are included in the article's Creative Commons licence, unless indicated otherwise in a credit line to the material. If material is not included in the article's Creative Commons licence and your intended use is not permitted by statutory regulation or exceeds the permitted use, you will need to obtain permission directly from the copyright holder. To view a copy of this licence, visit <http://creativecommons.org/licenses/by-nc-nd/4.0/>.

© The Author(s) 2025, corrected publication 2026